




Article

Spatially Resolved Source Apportionment of Industrial VOCs Using a Mobile Monitoring Platform

Robert M. Healy ^{*}, Uwayemi M. Sofowote, Jonathan M. Wang , Qingfeng Chen and Aaron Todd 

Environmental Monitoring and Reporting Branch, Ontario Ministry of the Environment Conservation and Parks, Toronto, ON M9P 3V6, Canada

* Correspondence: robert.healy@ontario.ca

Abstract: Industrial emissions of volatile organic compounds (VOCs) directly impact air quality downwind of facilities and contribute to regional ozone and secondary organic aerosol production. Positive matrix factorization (PMF) is often used to apportion VOCs to their respective sources using measurement data collected at fixed sites, for example air quality monitoring stations. Here, we apply PMF analysis to high time-resolution VOC measurement data collected both while stationary and while moving using a mobile monitoring platform. The stationary monitoring periods facilitated the extraction of representative industrial VOC source profiles while the mobile monitoring periods were critical for the spatial identification of VOC hotspots. Data were collected over five days in a heavily industrialized region of southwestern Ontario containing several refineries, petrochemical production facilities and a chemical waste disposal facility. Factors associated with petroleum, chemical waste and rubber production were identified and ambient mixing ratios of selected aromatic, unsaturated and oxygenated VOCs were apportioned to local and background sources. Fugitive emissions of benzene, highly localized and predominantly associated with storage, were found to be the dominant local contributor to ambient benzene mixing ratios measured while mobile. Toluene and substituted aromatics were predominantly associated with refining and traffic, while methyl ethyl ketone was linked to chemical waste handling. The approach described here facilitates the apportionment of VOCs to their respective local industrial sources at high spatial and temporal resolution. This information can be used to identify problematic source locations and to inform VOC emission abatement strategies.

Keywords: VOCs; source apportionment; mobile monitoring; fugitive emissions



Citation: Healy, R.M.; Sofowote, U.M.; Wang, J.M.; Chen, Q.; Todd, A. Spatially Resolved Source Apportionment of Industrial VOCs Using a Mobile Monitoring Platform. *Atmosphere* **2022**, *13*, 1722. <https://doi.org/10.3390/atmos13101722>

Academic Editor: Eduardo (Jay) Olaguer

Received: 13 September 2022

Accepted: 18 October 2022

Published: 20 October 2022

Publisher's Note: MDPI stays neutral with regard to jurisdictional claims in published maps and institutional affiliations.



Copyright: © 2022 by the authors. Licensee MDPI, Basel, Switzerland. This article is an open access article distributed under the terms and conditions of the Creative Commons Attribution (CC BY) license (<https://creativecommons.org/licenses/by/4.0/>).

1. Introduction

Volatile organic compounds (VOCs) are emitted from a variety of anthropogenic sources including on-road and off-road vehicles, personal care products, solvent use and industrial activities [1–3]. VOC emissions from these sources impact air quality locally but also contribute to ozone formation and secondary organic aerosol production at regional and transboundary scales [4–8]. Exposure to toxic VOCs, for example those classified as hazardous air pollutants and regulated by the USEPA, is associated with negative health outcomes, including increased cancer risk [9]. Minimizing anthropogenic VOC emissions to air is therefore beneficial from a public health perspective. Several countries, including the United States and Canada, have ratified the Gothenburg Protocol and its 2012 amendments which aim to reduce emissions of transboundary air pollutants including VOCs [10].

In Canada, the oil and gas sector is estimated to be the dominant source of anthropogenic VOCs nationally, contributing approximately 35% of total emissions, with the manufacturing sector (including petrochemical production) also associated with substantial emissions (7%) [11]. However, the impacts of these sectors on local ambient air quality differ greatly across the country as a function of proximity to operations [12–18]. Quantifying the relative contributions of different VOC sources at a specific location through

stationary measurements can be challenging, particularly in heavily industrialized areas where VOCs are emitted by several facilities. Positive matrix factorization (PMF) [19] is now frequently used to apportion VOCs measured at fixed receptor sites to local and regional sources and has been applied to continuous ambient VOC datasets in several countries, often with the aim of informing air quality policy decision-making [20–28]. However, the apportionment results are in many cases specific to the site selected for monitoring and therefore not necessarily representative of other locations, for example sensitive receptors, within the same region.

Here, we describe a method involving PMF analysis of a combination of mobile and stationary high frequency proton transfer time of flight mass spectrometry (PTR-ToF-MS) monitoring data and its application in apportioning VOCs to local sources at fine spatial scales. Stationary data are necessary to successfully extract source-specific factors while the mobile monitoring data are required to assess relative source contributions at a wide variety of receptor sites. We apply this technique to measurement data collected in the heavily industrialized city of Sarnia in southwestern Ontario which is home to over 40 industrial facilities including refining, petrochemical production and chemical waste disposal operations [29]. The spatially resolved apportionment results are combined with satellite imagery to both highlight VOC hotspots and to associate elevated concentrations with specific sources. The approach described here is expected to be a useful tool for informing VOC emission abatement actions in other industrialized regions where local air quality is impacted by a variety of VOC sources.

2. Materials and Methods

2.1. Monitoring Area

All monitoring took place in June 2020 in the city of Sarnia, the Aamjiwnaang First Nation Reserve and the township of St. Clair, which lie along the St. Clair River in southwestern Ontario, Canada, close to the United States border. This border region is the focus of the Michigan–Ontario Ozone Source Experiment (MOOSE) project, although the measurements described here took place one year prior to the 2021 intensive MOOSE field study period. Sarnia’s industrial zone is referred to colloquially as ‘Chemical Valley’ due to its high density of local chemical facilities [12,30]. Environment and Climate Change Canada’s (ECCC) national pollutant release inventory identifies 25 separate facilities reporting emissions of VOCs to air in the Sarnia/St. Clair area, with combined emissions of approximately 3700 tonnes annually [29]. Among the highest emitters are three oil refineries, several petrochemical production facilities and a chemical waste treatment/disposal facility.

2.2. Mobile Monitoring Platform

An Ontario Ministry of the Environment, Conservation and Parks (MECP) mobile monitoring platform was used for all stationary and mobile VOC measurements. The platform, shown in Figure S1, is comprised of a cab-over truck and an air-conditioned cargo box customized to house a suite of air monitoring instrumentation. An on-board global positioning system (GPS) was used to record location data at 5 s resolution. A meteorological sensor (AIO2, Met One Instruments, Grants Pass, OR, USA) fixed to a telescopic tower was used to measure wind speed, wind direction, ambient temperature and relative humidity at 5 s resolution. While the vehicle was stationary, the tower was raised to a height of approximately 10 m above ground level (AGL) to enable accurate measurement of wind speed and wind direction, facilitating VOC source identification. While mobile, the telescopic tower was lowered, precluding measurement of wind speed and direction. Supporting wind speed and wind direction data from a local MECP air quality station (42.990263° N, 82.395341° W) were used for those periods when the vehicle was moving. VOCs were measured at 5 s resolution using an on-board proton transfer reaction time-of-flight mass spectrometer (PTR-ToF-MS 8000, Ionicon Analytik GmbH, Innsbruck, Austria). The mobile platform also contains instrumentation for real-time

monitoring of common air pollutants including NO/NO_x (Model 42c, Thermo Scientific, Waltham, MA, USA), O₃ (Model O342e, Environnement S.A., Poissy, France), SO₂ (Model 43i TLE, Thermo Scientific), PM_{2.5} and PM₁₀ (Model T640 PM Mass Monitor, Teledyne API, San Diego, CA, USA), although only the VOC measurement data will be discussed here.

2.3. PTR-ToF-MS Measurements

The PTR-ToF-MS model used here is described in detail elsewhere [31]. Briefly, H₃O⁺ reagent ions were generated using a hollow cathode ion source and mixed with sampled ambient air in a drift tube facilitating proton transfer to the neutral VOCs. Protonated VOCs were subsequently transmitted to a time-of-flight mass spectrometer for detection. Ambient air was pumped through an inlet extending from the roof of the vehicle (3.5 m AGL) at a flow rate of 100 L min^{−1} through a 1 in diameter glass sampling line. The PTR-ToF-MS sampled air at 100 mL min^{−1} from the main flow through 1/16 in diameter PEEK tubing. A particle filter (SS-4F-15, Swagelok) was used to prevent transmission of ambient particulate matter to the PTR-ToF-MS. The residence time for VOCs in the inlet system prior to entering the PTR-ToF-MS was approximately 2 s. The PTR-ToF-MS was operated with a drift region pressure of 2.30 mbar, a drift region temperature of 80 °C and a drift field (E/N ratio) of 140 Td. Mass spectral data were acquired and processed at 5 s resolution.

The MECP mobile platform is predominantly used for industrial non-compliance surveys and therefore calibrations were performed for common air toxics expected to be observed during industrial monitoring deployments. The PTR-ToF-MS was calibrated directly using two certified standard cylinders containing mixtures of VOCs in nitrogen (Praxair Inc., Danbury, CT, USA, uncertainty 10%) diluted using humidified zero air. The first cylinder contained a mixture of 1 ppm each of benzene, toluene, styrene, *m*-xylene, ethylbenzene, 1,2,4-trimethylbenzene, naphthalene, 1,3-butadiene, propene, butene, vinyl chloride, chlorobenzene, trichloroethylene, tetrachloroethylene and hexachlorobutadiene. The second cylinder contained a 1 ppm mixture of acetone, acetaldehyde, vinyl acetate, methyl ethyl ketone (MEK), methyl isobutyl ketone (MIBK) and phenol. All species were quantified using their respective MH⁺ responses exclusively. The PTR-ToF-MS cannot differentiate between xylenes and ethylbenzene, and the latter fragments more extensively than the former upon ionization. Thus, the sensitivity used to quantify C₂ aromatics at m/z 107 in this work lies between that of *m*-xylene and ethylbenzene. Not all of the species for which calibrations were performed were included in the positive matrix factorization (PMF) analysis, as discussed below. Zero measurements were performed using humidified zero air at the beginning of the study period. All ambient monitoring data were collected over five days in June 2020 (16, 17, 18, 23 and 24 June). Stationary sampling was performed at locations characterized by highly elevated VOC concentrations, identified while performing mobile monitoring each day. 78% (27.5 h) of the PTR-ToF-MS dataset was collected while stationary and 22% (7.9 h) was collected while mobile. All measurements took place between 9 AM and 8 PM local time. The average speed of the monitoring platform while mobile was 59 km/h, providing an average spatial data resolution of approximately 250 m. At times the vehicle was driven at much lower speeds however, particularly when higher VOC signals were observed near major sources, which provided finer spatial resolution.

2.4. PTR-ToF-MS Data Processing and PMF Analysis

In order to perform untargeted PMF analysis of the PTR-ToF-MS dataset, unit mass resolution data were used. Signals were integrated between -0.4 and $+0.4$ Th for each nominal m/z in the range 30–300 using PTR Viewer software (Ionicon Analytik GmbH) and normalized using the signal for H₃¹⁸O⁺ at m/z 21, producing normalized counts per second (ncps) data to mitigate changes in hydronium ion concentration and instrument sensitivity as a function of time [21]. Zero air measurement data were processed in the same way and zero signals were subtracted from the ambient dataset signals. Selected ions with known instrumental interferences were removed from the data matrix prior to PMF analysis (m/z 30, 32, 34–39 and 55) [21].

PMF is a factor analysis algorithm that can be applied to temporally resolved monitoring datasets to apportion measured chemical species to their respective sources. PMF reconstructs the measurement data matrix as a linear sum of a user-defined number of factor profiles with contributions that vary with time. PMF analysis of PTR-MS datasets has been performed previously in a variety of locations globally, typically for longer term stationary datasets [21,32–36], although some applications to mobile laboratory data are recently beginning to emerge [28,37]. The PTR-ToF-MS zero-corrected ambient mass spectral data were analyzed using the EPA PMF 5.0 program [38], which solves the bilinear factor analytical equation (Equation (1)) using the Multilinear Engine (ME-2) [39]:

$$X = GF + E \quad (1)$$

where X is the input data matrix, G is the left-side or factor contribution matrix, F is the right-side or factor profile matrix and E is the residual matrix to be minimized. The uncertainties of the ion counts from the PTR-ToF-MS were assumed to be approximated by a Poisson distribution [37,40]. The data and uncertainty matrices at 5 s sampling resolution consisted of over 25,000 rows and were subsequently averaged to 15 s resolution to yield matrices that were more manageable computationally for the PMF program. The EPA PMF program allows for variables to be ranked as ‘strong’, ‘weak’ or ‘bad’ based on their signal-to-noise ratio (S/N). These classes differ in the way their respective uncertainties are treated during matrix factorization to prevent overfitting and generation of unreliable factors. The default criteria were unrealistic for this study given the sporadic nature of source sampling, and therefore the following criteria were developed: ‘strong’ variables were defined as those with $S/N \geq 0.3$ (18 ions), ‘weak’ variables were those with $0.3 > S/N \geq 0.1$, or $S/N < 0.1$; $\max \text{ncps} \geq 4.0$ (44 ions), and ‘bad’ variables were those with $S/N < 0.1$; $\max \text{ncps} < 4.0$ (202 ions). Thus, 62 ions were retained for PMF analysis in this study. Because the PTR-ToF-MS measurement uncertainties are only approximately Poisson-like in distribution, extra modelling uncertainty was required to fully capture the errors associated with the ions used, and final values of 0.2 were added to the input errors. The use of seven factors was found to be optimal and a detailed description of the PMF analysis and optimization [41] is provided in the Supporting Information (Figures S2–S9 and Tables S1–S4).

3. Results

3.1. PMF Results

The reconstructed total ion signal for the final seven-factor PMF solution agreed very well with the measured total PTR-ToF-MS ion signal ($R^2 = 0.99$, slope = 0.98), as shown in Figure S9. Four of the seven factors resolved through PMF were associated with local emissions due to their high temporal and spatial variability (Factors 1, 2, 3 and 4). The three remaining factors exhibited much lower spatial and temporal variability and were therefore associated with regional/background sources (Factors 5, 6 and 7). The mass spectral factor profiles and factor contribution temporal trends for the four local factors are shown in Figures 1 and 2, respectively. The three background factor profiles and contribution temporal trends are shown in Figures S10 and S11, respectively.

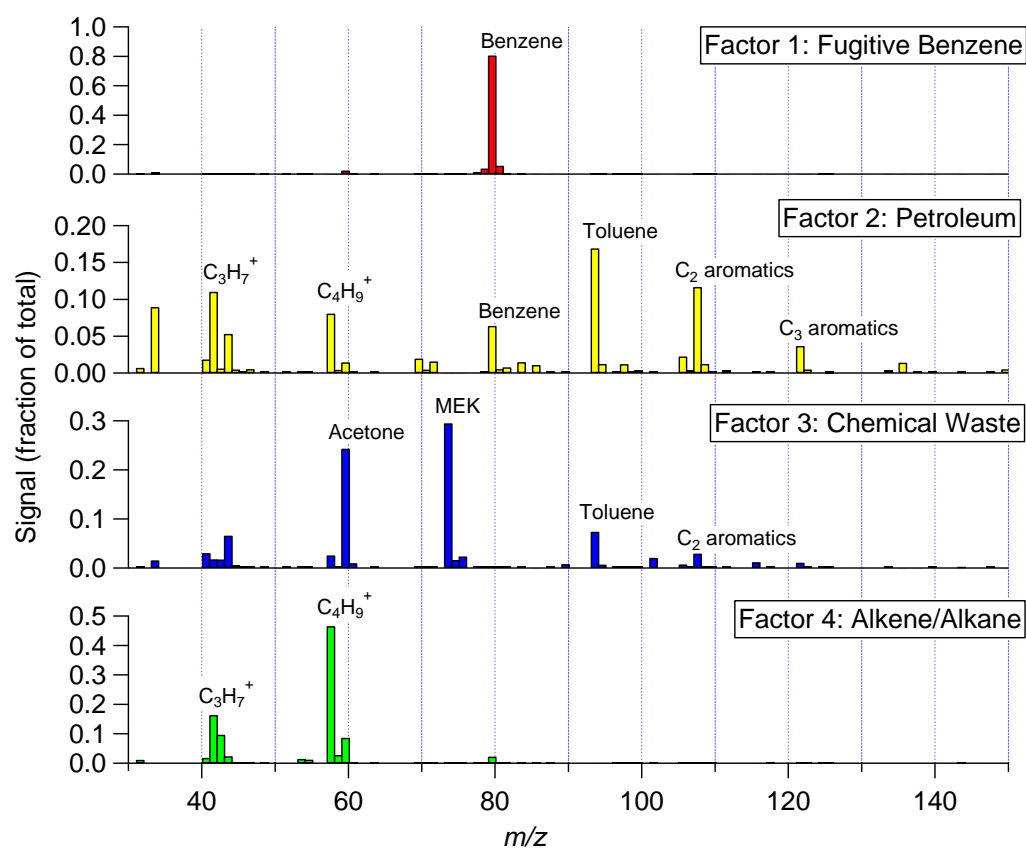


Figure 1. Mass spectral profiles for the four local factors.

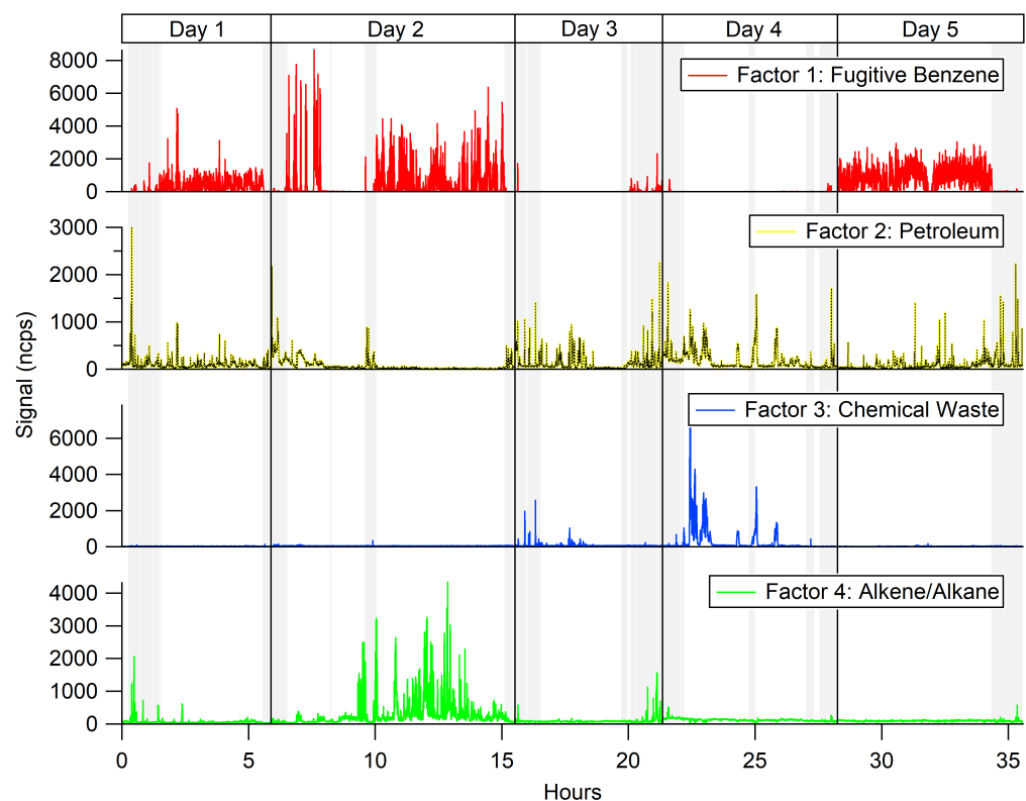


Figure 2. Temporality of factor contributions for the four local factors. Mobile monitoring periods are highlighted in grey and stationary monitoring periods are indicated by a white background.

The mass spectral profile for Factor 1 (termed Fugitive Benzene) is dominated by a signal for benzene at m/z 79, with minimal input from other ions. This profile is indicative of sources that emit benzene without substantial concurrent emissions of other VOCs. Factor 2 (termed Petroleum) is dominated by aromatic hydrocarbon ions (benzene, toluene, C_2 and C_3 aromatics), and aliphatic hydrocarbon fragment ions ($C_3H_5^+$, $C_4H_9^+$), consistent with a petroleum fuel signature [42]. Similar PTR-MS mass spectral signatures have been previously observed in ambient air impacted by vehicular exhaust and downwind of petroleum production activities [7,14,22,24,28,43]. Factor 3 (termed Chemical Waste) is characterized by a more unusual combination of VOCs: acetone, methyl ethyl ketone (MEK), toluene and C_2 aromatics. This signature is consistent with emissions from a chemical waste and disposal facility in the study area that handles waste from a variety of industrial sources in Canada and the United States. Emissions of VOCs from this facility have been characterized previously using mobile monitoring platforms equipped with triple-quadrupole mass spectrometers [44]. Finally, Factor 4 (termed Alkene/Alkane) is characterized by a dominant signal at m/z 57. This ion can represent protonated butene ($C_4H_8 \cdot H^+$), for which a calibration was performed, but can also represent a fragment ion of both linear and branched alkanes ($C_4H_9^+$). While the PTR-ToF-MS does not efficiently quantify alkanes due to their relatively low proton affinities, ionization and subsequent fragmentation of these species can lead to significant positive interferences at m/z 57 [7,14,42]. A smaller signal is also apparent in the factor profile at m/z 43, corresponding either to protonated propene ($C_3H_6 \cdot H^+$), for which a calibration was also performed, or a fragment ion of linear or branched alkanes ($C_3H_7^+$). Additional contributions from fragmentation of oxygenated species at m/z 43 ($C_2H_3O^+$) are also possible.

Figure 2 highlights the strong variability in signal contributions for the four local factors as a function of time over the five days of monitoring. Stationary measurements were performed, in some cases for several hours at a time, at locations where elevated VOC concentrations were detected while driving. As shown in Figure 2, the highest signals were typically observed while stationary. For Day 1, Day 2 and Day 5, stationary measurements were mostly performed at locations impacted by elevated benzene concentrations (Factor 1), shown in Figure S13 and Table S5. On Day 3 and Day 4, stationary monitoring was performed at locations where elevated MEK and acetone were observed (Factor 3), shown in Figure S14 and Table S6. The highest signals for butene/ $C_4H_9^+$ (Factor 4) were observed on Day 2, during the same period when high signals for Factor 1 were also observed, although the temporality of the two factors was very different, indicative of separate local sources. In contrast to the other three local factors, elevated signals for Factor 2 were observed on all five days of the study. To identify likely local sources that may be contributing to elevated signals for the four local factors, examination of the spatial distributions of the factor contributions was undertaken. No obvious diurnal patterns were observed for the factor contributions, with proximity to major sources driving temporality for the local factors rather than changes in emissions as a function of time of day due to the nature of the mobile monitoring activities.

A factor for volatile chemical product (VCP) emissions was not identified through PMF analysis in this work. Emissions of VCPs, particularly in urban areas characterized by high population density, have recently been demonstrated to be an important source of VOCs, and can dominate over vehicular emissions of VOCs in densely populated cities [28]. Ions associated with VCP use [3], including ethanol (m/z 47), texanol (m/z 199) and octamethylcyclotetrasiloxane (m/z 297), were classified as 'bad' variables, indicating either poor signal-to-noise or very low concentrations, and thus were not included in the PMF analysis. While the marker ion for decamethylcyclopentasiloxane (m/z 371) was not formally considered for the PMF analysis as a variable, manual examination of the temporality of the signal did not reveal any variability indicative of local sources or concentration gradients. The lower importance of VCP emissions relative to industrial emissions of VOCs in the study area is likely a reflection of land use. Sarnia is a relatively small city, with a population of approximately 70,000 inhabitants, and the majority of

the monitoring was performed to the south of the city, where population density is low and industrial activities dominate land use, as well as rural areas further to the east and south. Some relevant ions with the potential for contribution from VCP emissions that were included in the PMF analysis are m/z 137 (limonene, pinenes) and m/z 161 (para-chlorobenzotrifluoride), but both ions exhibited low signals and were associated predominantly with the background factors, indicative of regional contributions rather than local emissions.

3.2. Spatially Resolved Apportionment: Local Factor Contributions

Figure 3 shows the signal contributions for the four local factors as a function of location for the entire study period. Only mobile monitoring periods are included in this spatial map for clarity because the signal contributions observed while stationary were extremely high at times. Geospatial data visualizations were created using Tableau Desktop (version 2021.3.1, Tableau Software, Seattle, WA, USA). In Figure 3, the position of each pie chart denotes the measurement location for a given 15 s measurement period, the diameter of the pie chart corresponds to the summed signal contributions of the four local factors for that measurement period, and the wedge sizes represent the relative signal contributions from each factor. Industrial facilities along the mobile monitoring routes are also labeled, including the three major refineries in the area, several chemical/petrochemical production/storage facilities, and the single major waste disposal facility. Upon examination of the spatial distribution of the factor contributions in Figure 3, some patterns are apparent. Contributions for Factor 1 (Fugitive Benzene) are dominant in a relatively small region in the northwest of the study area, close to a refinery and a cluster of five chemical facilities. This area has previously been demonstrated to feature the highest ambient VOC concentrations in Sarnia through the deployment and off-line analysis of passive samplers [12]. Contributions for Factor 3 (Chemical Waste) are most dominant in the southeast of the study area, close to the single chemical waste facility. While higher contributions for Factor 2 (Petroleum) are observed in the vicinity of the three refineries along the St. Clair River, there are lower, but significant, contributions throughout the rest of the study area. This indicates that sources other than refining, most likely predominantly vehicular traffic, are also likely to be important contributors to Factor 2. The relative contributions from refining and traffic unfortunately cannot be separated in this work, and both sources are observed to contribute to elevated toluene and aromatic VOC mixing ratios across the study area. Longer term fixed site monitoring data would be better suited to effectively separating and quantifying the overall relative contributions of these two sources to local ambient VOC levels. As with Factor 1, the highest contributions for Factor 4 (Alkene/Alkane) are observed in the northwest of the study area, although lower contributions are also observed throughout the study area, similar to Factor 2, suggesting a potential influence of traffic-related or background alkanes/alkenes.

While examination of the relative total ion signal contributions of the local factors is helpful in the identification of VOC source areas, it is also useful to investigate the relative contributions of the local factors to mixing ratios of specific VOCs. Although the PTR-ToF-MS was directly calibrated for a range of VOCs, we focus on four VOCs here based on their dominant contributions to the different mass spectral profiles shown in Figure 1; namely benzene (Factor 1), toluene (Factor 2), MEK (Factor 3) and butene (Factor 4).

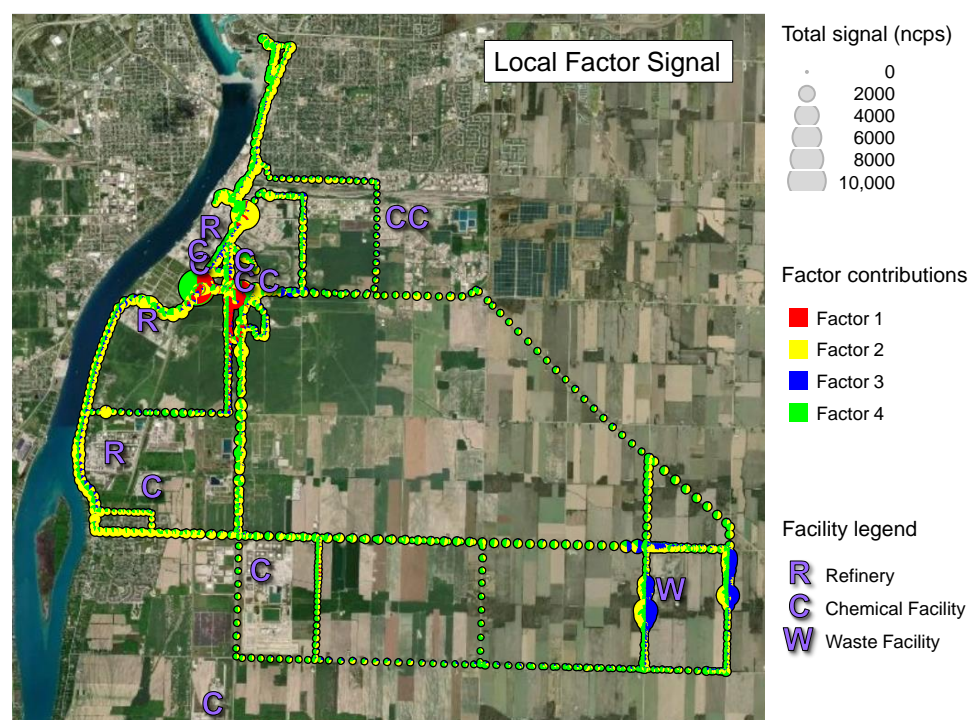


Figure 3. Relative PTR-ToF-MS signal contributions of each of the four local factors as a function of measurement location while mobile. The diameter of each pie denotes the total summed signal of the four local factors for a given measurement period and the size of each wedge within each pie represents the relative contribution of each factor for that measurement period.

3.3. Spatially Resolved Apportionment: Benzene

As shown in Figure 4, very strong spatial gradients for benzene were observed across the study area, with mixing ratios of up to almost 60 ppb associated with local factors measured at times while mobile. The highest mixing ratios were observed in the northwest, close to the northernmost refinery and a cluster of chemical facilities. In contrast, mixing ratios were much lower throughout the remainder of the study area, especially in the rural areas furthest from industrial sources (<0.1 ppb at times).

Figure 5 features a zoomed-in view of the region where the highest benzene mixing ratios were observed, focusing on a single short mobile monitoring period (26 June 2020 14:10–14:45) to better highlight the influence of specific local sources. Wind was from the north at the time. While driving around the northeast perimeter of the main refinery site, elevated benzene mixing ratios up to approximately 6 ppb were observed, dominated by contributions from Factor 2 (Petroleum), consistent with the expected VOC profile from petroleum production. Interestingly, a separate contribution from Factor 1 (Fugitive Benzene) was also observed while passing a storage tank area located in the northeast corner of the refinery site. While driving southward, beyond the refinery, benzene mixing ratios decreased significantly, but then sharply increased again while downwind of a storage tank area at the southwesternmost chemical facility. This is a petrochemical storage facility that contains a dedicated benzene storage tank, and the elevated Factor 1 contributions to benzene at this location are most likely attributable to that specific source. While moving eastward from that facility, significant Factor 1 contributions to benzene mixing ratios were again observed downwind of another tank area at the south end of the central southern petrochemical facility. This tank area also contains a dedicated benzene storage tank that is likely responsible for the elevated benzene mixing ratios observed. The benzene gradients observed here, as well as the dominance of fugitive emissions, highlight the value of mobile fenceline monitoring to aid in identifying point or area sources that contribute to elevated mixing ratios of hazardous VOCs downwind.

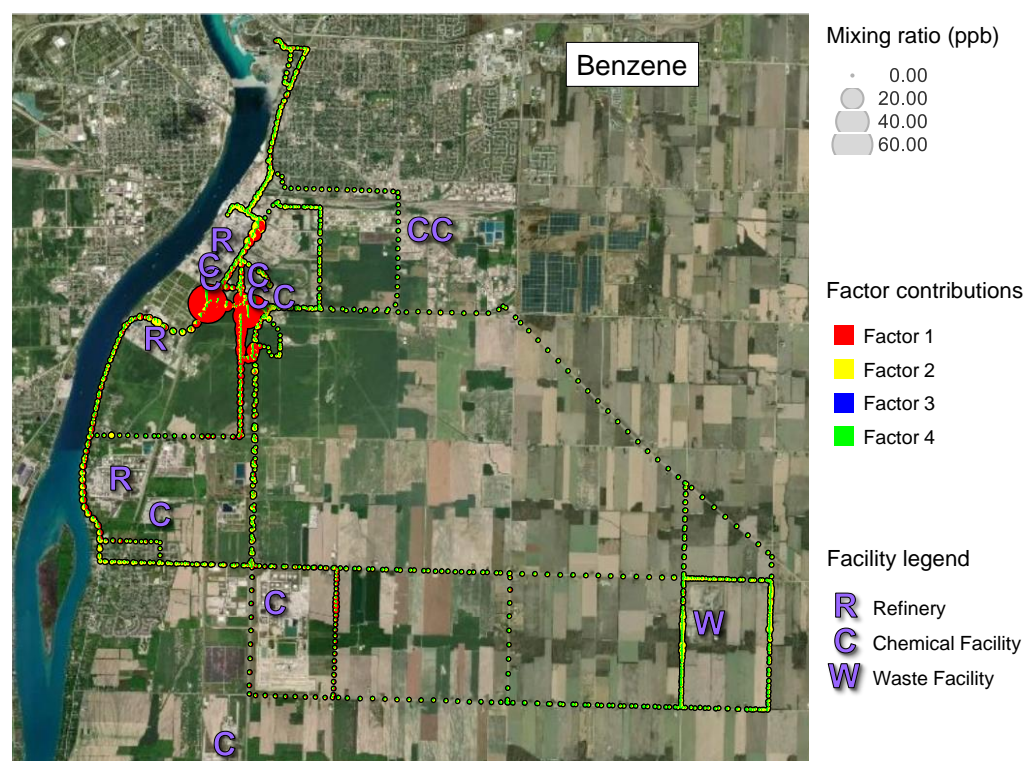


Figure 4. Contributions of each of the four local factors to benzene mixing ratios as a function of measurement location while mobile. The diameter of each pie denotes the benzene mixing ratio and the size of each wedge within each pie represents the relative contribution of each factor for that measurement period.

3.4. Spatially Resolved Apportionment: Toluene

The spatial distribution of toluene associated with the four local factors is very different to that observed for benzene, as shown in Figure 6. Enhancements in toluene mixing ratios (up to almost 15 ppb) are apparent in the vicinity of the three local refineries located along the St. Clair River, and contributions from Factor 2 (Petroleum) are highly dominant throughout the western part of the study area. While it is expected that elevated toluene would be observed in close proximity to refining operations, with the three refinery sites combined estimated to emit approximately 100 tonnes annually [28], there is also a persistent contribution from Factor 2 to toluene mixing ratios along most of the roadways investigated. This highlights the influence of local vehicular traffic on toluene mixing ratios throughout the study area. The only region where contributions from Factor 2 to ambient toluene are not wholly dominant is the southeastern corner of the study area, where contributions from Factor 3 (Chemical Waste) also become relevant. A major chemical waste facility is located here which reports emissions of approximately 30 tonnes of toluene to air annually [28] and is confirmed as a significant source of toluene here through mobile monitoring.

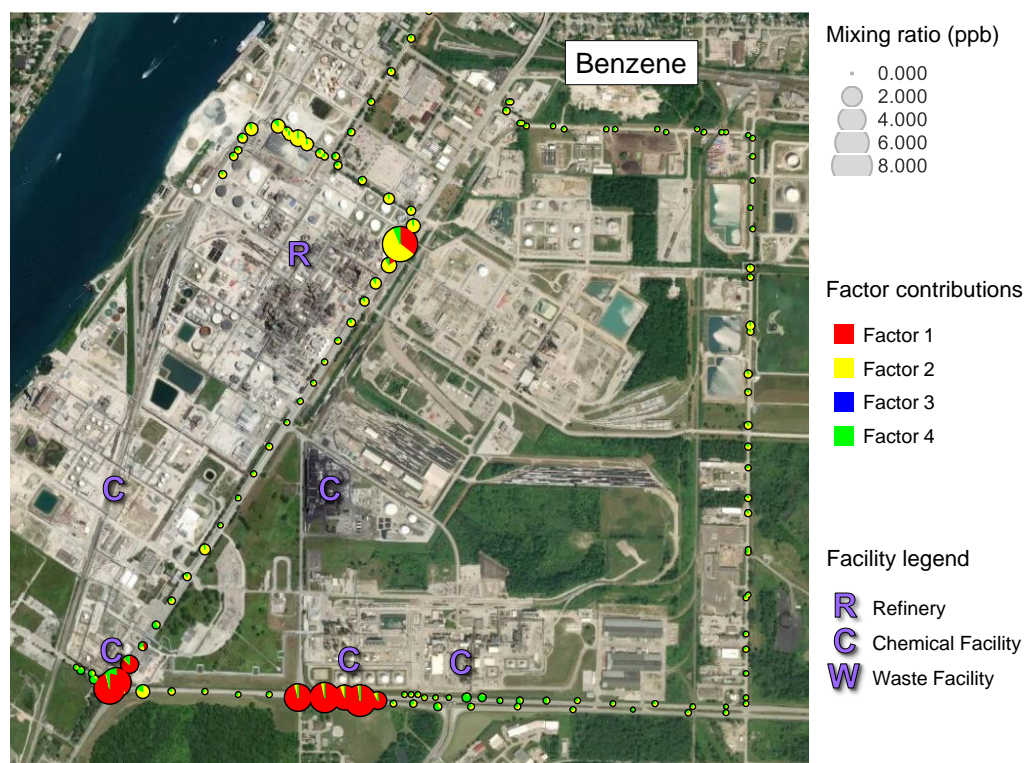


Figure 5. Contributions of each of the four local factors to benzene mixing ratios as a function of measurement location while mobile on 16 June 2020, 14:10–14:45. Wind was northerly at the time. The diameter of each pie denotes the benzene mixing ratio and the size of each wedge within each pie represents the relative contribution of each factor for that measurement period.

3.5. Spatially Resolved Apportionment: MEK

The spatial distribution of MEK mixing ratios, and the relative local factor contributions, are again very different to those observed for benzene and toluene. As shown in Figure 7, Factor 3 (Chemical Waste) is the dominant contributor to MEK. The highest mixing ratios (up to almost 15 ppb) were observed in the southeast, where the single local chemical waste disposal facility, also responsible for elevated toluene ambient mixing ratios, is located. This facility is estimated to release approximately 12 tonnes of MEK annually [29] and emissions of MEK from this site have also been detected downwind previously using a different mobile monitoring platform [44]. The chemical waste facility is the single major source of MEK identified through mobile monitoring in the study area.

3.6. Spatially Resolved Apportionment: Butene

Estimating butene mixing ratios using the PTR-ToF-MS is challenging because of the potential for interference at m/z 57 from fragmentation of ambient alkanes [7,42]. This is particularly problematic for the Sarnia area, where intensive refining operations result in relatively high mixing ratios of alkanes relative to other parts of Ontario. Alkanes (and a wide range of other VOCs) are routinely quantified using 24-h canister deployments at a local air quality station (42.912545, −82.416816) under ECCC's National Air Pollutant Surveillance Program [45]. In 2019 the annual mean concentrations of propane, butane, pentane and hexane (4.1, 4.7, 3.4 and 2.8 $\mu\text{g m}^{-3}$, respectively) measured at the station were much higher than concentrations of propene and butene (1.2 and 0.8 $\mu\text{g m}^{-3}$, respectively). Thus, while local contributions of propene and butene are indeed expected to contribute to the PTR-ToF-MS signals at m/z 43 and 57, substantial positive interferences from linear and branched alkanes are also expected. The ambient mixing ratios of butene shown in Figure 8 should therefore be considered only as possible upper limits. Unlike toluene, which was characterized by reasonably similar mixing ratio enhancements near all three refineries, the

highest butene mixing ratios were observed in the northwest of the study area, near the northernmost refinery and the cluster of five chemical facilities.

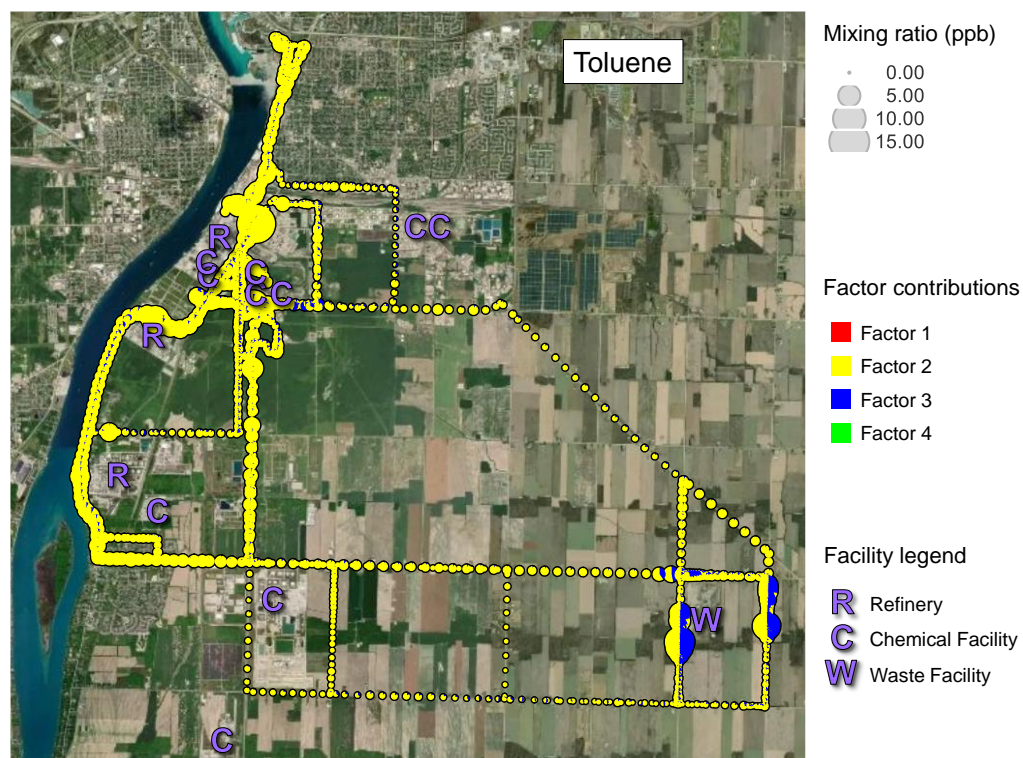


Figure 6. Contributions of each of the four local factors to toluene mixing ratios as a function of measurement location while mobile. The diameter of each pie denotes the toluene mixing ratio and the size of each wedge within each pie represents the relative contribution of each factor for that measurement period.

Figure 9 features a zoomed-in view of this region focusing on the mobile monitoring period of 17 June 2020, 13:10–13:35, when wind was from the north. While driving downwind of the refinery site, which reports annual butene emissions of 27 tonnes [29], elevated butene levels were observed, dominated by contributions from Factor 4 (Alkene/Alkane) but with some contribution from Factor 2 (Petroleum). However, the highest butene mixing ratios, completely dominated by contributions from Factor 4, were observed while downwind of the two chemical facilities shown in the southwest corner of Figure 9. The more northerly of these two is a rubber production facility, which reports annual butene emissions of approximately 6 tonnes annually [29]. The wind dependence [46] of the highest butene levels measured while stationary on 17 June confirms this facility as the most likely source (Figure S15). Elevated butene was also measured directly downwind of the southeasternmost chemical facility shown in Figure 9, another rubber production site, which reports annual butene emissions of 7 tonnes [29]. While interferences from alkanes do limit the accuracy of the estimated butene mixing ratios, the locations of the hotspots identified through mobile monitoring are consistent with reported butene emissions data.

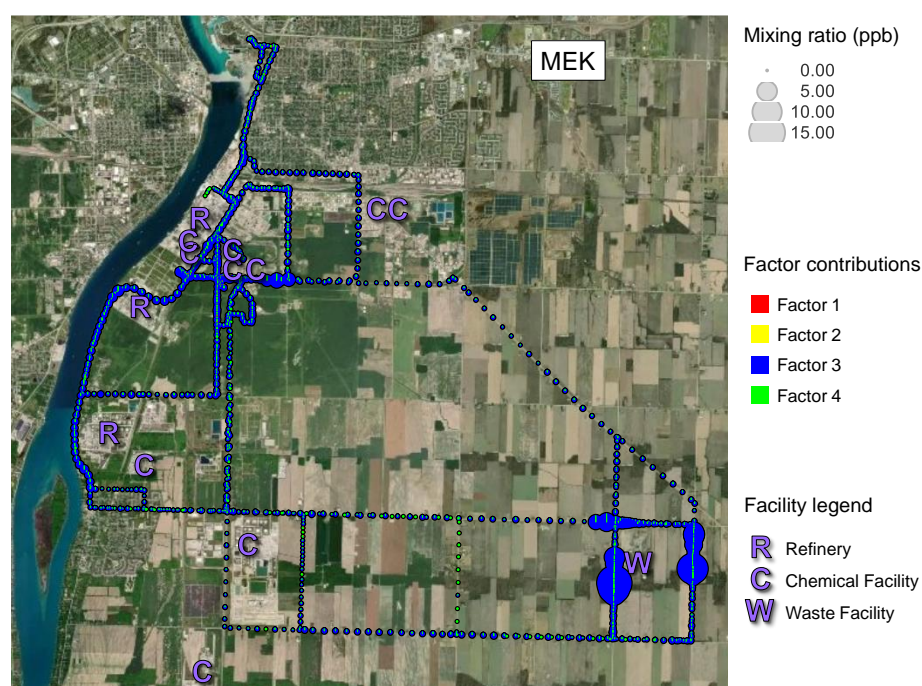


Figure 7. Contributions of each of the four local factors to MEK mixing ratios as a function of measurement location while mobile. The diameter of each pie denotes the MEK mixing ratio and the size of each wedge within each pie represents the relative contribution of each factor for that measurement period.

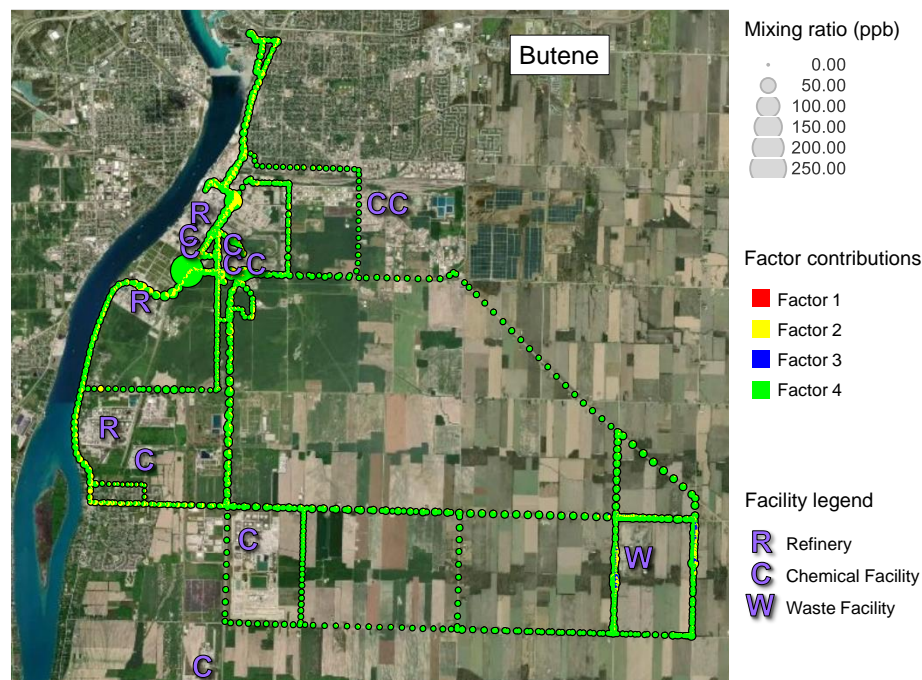


Figure 8. Contributions of each of the four local factors to butene mixing ratios as a function of measurement location while mobile. The diameter of each pie denotes the butene mixing ratio and the size of each wedge within each pie represents the relative contribution of each factor for that measurement period. It is important to note that reported butene mixing ratios should be considered as an upper limit due to interferences at m/z 57 from the fragmentation of alkanes.

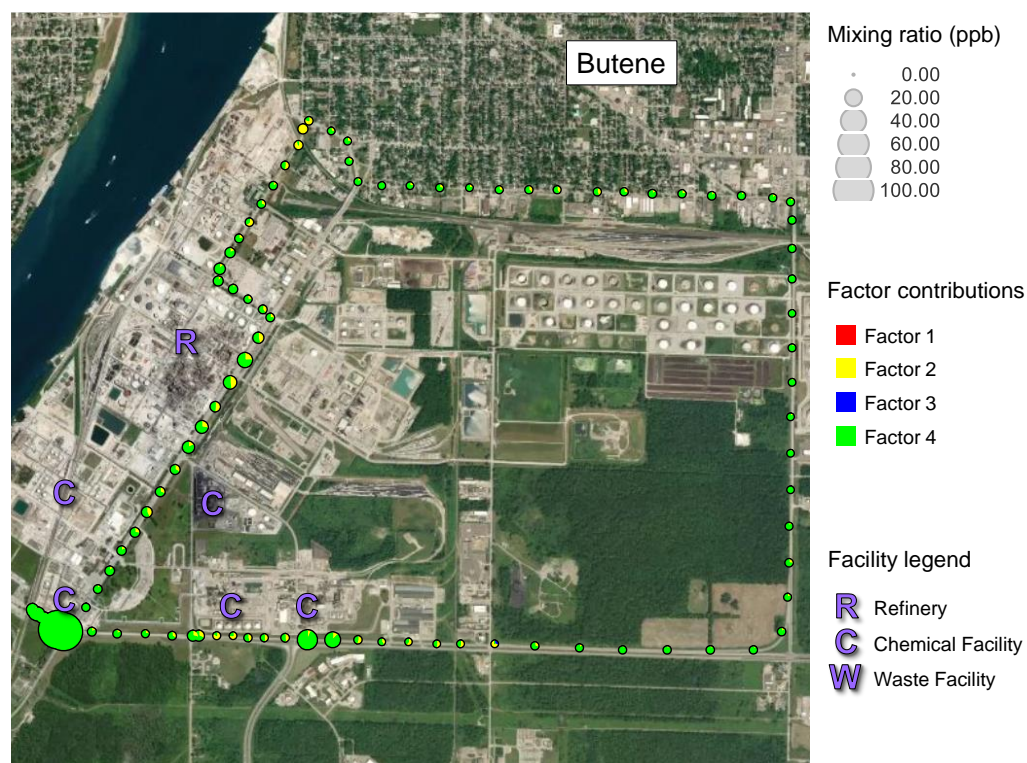


Figure 9. Contributions of each of the four local factors to butene mixing ratios as a function of measurement location while mobile on 17 June 2020, 13:10–13:35. Wind was northerly at the time. The diameter of each pie denotes the butene mixing ratio and the size of each wedge within each pie represents the relative contribution of each factor for that measurement period. It is important to note that reported butene mixing ratios should be considered as an upper limit due to interferences at m/z 57 from the fragmentation of alkanes.

3.7. Overall Source Apportionment Results

Results for the apportionment of the most abundant measured VOCs to the four local factors and to background sources (Factors 5, Factor 6 and Factor 7 combined) while mobile are shown in Figure 10 and Table 1. Only mobile monitoring periods are considered here because inclusion of periods when the vehicle was stationary biases the apportionment results towards the monitoring locations selected, which were in most cases very close to the major local industrial VOC sources (for comparison these results are provided in Figure S16 and Tables S7 and S8). Considering the data collected across the entire study area while mobile provides a more representative picture of the relative contributions of the different source sectors to ambient air quality in Sarnia.

Of the major polar oxygenated species measured by the PTR-ToF-MS, methanol, acetaldehyde and acetone, all exhibit minimal contributions from local sources and are instead characterized by dominant contributions from the regional background. The association of these species with oxidized regional background air is consistent with previous VOC source apportionment studies [21,22,24,37,47,48]. In contrast to the other oxygenated species, MEK is associated predominantly with local emissions, with a 54% contribution from Factor 3 (Chemical Waste), while the remainder is apportioned to the regional background. Butene is also apportioned predominantly to local emissions, with a 69% contribution from Factor 4 (Alkene/Alkane) attributable at least in part to local rubber production activities identified through spatial analysis, and a 16% contribution from Factor 2 (Petroleum). With the exception of benzene, ambient aromatic VOC mixing ratios are apportioned mostly (>60%) to Factor 2 (Petroleum), with contributions from both refining and vehicular traffic apparent in the spatial distribution data, although smaller contributions (<11%) from Factor 3 are also present. The highest contributor

to ambient benzene mixing ratios is Factor 1 (Fugitive Benzene), with a contribution of 48%, which is much higher than the local contribution from Factor 2 (16%). This result highlights that, to a large extent, local benzene emissions are decoupled from general petroleum emissions, with fugitive emissions from benzene storage and handling playing an important role. This is a particularly relevant finding considering the carcinogenicity of this species [49], and highlights the value of spatially resolved source apportionment in complex industrial airsheds.

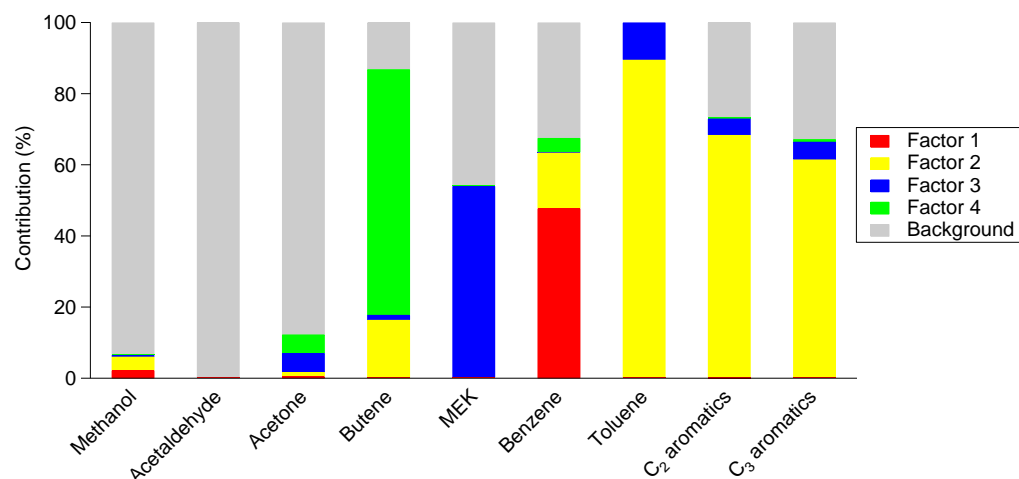


Figure 10. Apportionment of selected VOCs to the four local factors and the combined background factors averaged for periods when the vehicle was moving.

Table 1. Apportionment of selected VOCs to the four local factors and the combined background factors averaged for periods when the vehicle was moving.

	Factor 1	Factor 2	Factor 3	Factor 4	Background
Methanol	2.2	3.9	0.4	0.0	93.5
Acetaldehyde	0.0	0.0	0.0	0.0	100.0
Acetone	0.5	1.2	5.3	5.2	87.7
Butene	0.0	16.4	1.4	69.1	13.1
MEK	0.2	0.0	53.8	0.2	45.8
Benzene	47.7	15.7	0.1	4.1	32.5
Toluene	0.1	89.4	10.5	0.0	0.0
C ₂ aromatics	0.3	68.0	4.6	0.4	26.6
C ₃ aromatics	0.2	61.3	5.0	0.8	32.8

4. Conclusions

A combination of mobile PTR-ToF-MS monitoring and PMF analysis is demonstrated here to be a useful approach both for the identification of VOC hotspots and the apportionment of individual VOCs to local and regional sources. In the Sarnia study area investigated, four local factors were resolved through PMF analysis using five days of high time-resolution monitoring data collected both while stationary and mobile. These chemically distinct factors were characterized by signal contributions with high temporal and spatial variability. Geospatial mapping of VOC mixing ratios and factor contributions was also found to be helpful in the identification of the most likely source locations. While methanol, acetaldehyde and acetone were associated almost entirely with regional background sources, MEK, butene, benzene, toluene and substituted aromatics were found to be predominantly associated with local emissions. The spatial patterns for mixing ratios of the most abundant VOCs differed greatly, highlighting both the heterogeneity of exposure potential and the importance of correctly identifying the dominant sources (or source sectors) of different VOCs when designing effective abatement strategies. Substituted aromatics were associated predominantly with local refinery and vehicular traffic emissions,

MEK was associated with a single major chemical waste facility, benzene was associated predominantly with fugitive emissions from storage/handling, and the highest butene mixing ratios were linked to local rubber production facilities. Thus, entirely different targeted abatement actions would be required to reduce local emissions of each of these species. Heavily industrialized areas are often characterized by a high density of separate VOC emission sources, and deconvoluting contributions from individual facilities can be challenging, even when long term fixed site VOC measurement data are analyzed using PMF. The methodology described here is expected to be a useful tool for the separation of source sector contributions to ambient VOC mixing ratios at fine spatial scales in other industrial multi-source airsheds globally. Advantages include the extraction of spatially resolved source contributions under specific meteorological conditions and the identification of major local VOC sources. One drawback is that the shorter measurement period involved can be considered as being less representative of overall air quality in the study area when compared to more traditional long-term fixed-site measurements and apportionment. Long-term continuous monitoring likely remains a better option for quantifying local and regional contributions to ambient VOC mixing ratios at a specific single location over multiple seasons or years.

Supplementary Materials: The following supporting information can be downloaded at: <https://www.mdpi.com/article/10.3390/atmos13101722/s1>, Figure S1: MECP mobile monitoring platform interior and exterior; Figure S2: Reduction in Q with increasing factor number; Figure S3: Q/Q_{exp} for the factor profiles (top) and their summed contributions to total ion counts (bottom) for the base seven-factor solution; Figure S4: Stacked screenshots of the final constrained 7FS run showing no factor swaps in DISP and BS-DISP runs after the application of the final single constraint; Figure S5: Q/Q_{exp} for the factor profiles (top) and their summed contributions to total ion counts (bottom) for the final constrained seven-factor solution; Figure S6: Average factor contributions to total ion counts (ncps) for the base (left) and constrained (right) seven-factor solutions; Figure S7: Factor contributions to total ion counts (ncps) for each m/z for the base seven-factor solution; Figure S8: Factor contributions to total ion counts (ncps) for each m/z for the final constrained seven-factor solution; Figure S9: Relationship between reconstructed total ion signal and measured total ion signal for the final constrained seven-factor solution; Figure S10: Mass spectral profiles for the three background factors; Figure S11: Temporality of factor contributions for the three background factors. Mobile monitoring periods are highlighted in grey and stationary monitoring periods are indicated by a white background; Figure S12: Temporality of the factor contribution for Factor 7 and ambient relative humidity (top) and linear regression of the factor contribution for Factor 7 and ambient relative humidity (bottom); Figure S13: Stationary monitoring locations used on Days 1, 2 and 5; Figure S14: Stationary monitoring locations used on Days 3 and 4; Figure S15: CPF plot illustrating the dependence of the highest signals (>75th percentile) measured for butene (green) and benzene (red) upon wind direction while stationary at Site A on Day 2; Figure S16: Apportionment of selected VOCs to the four local factors and the combined background factors for the entire study period (stationary and mobile) (top) and for stationary periods only (bottom); Table S1: PMF input statistics for the retained zero-background subtracted ions (ncps units); Table S2: Model fits for all ions used in the PMF analyses; Table S3: Scaled residuals beyond 3 standard deviations (dates by species); Table S4: Error estimation summary (BS, DISP, BS-DISP) for the base model. Note that factor swaps were present in the BS-DISP results; Table S5: Stationary monitoring details for Days 1, 2 and 5; Table S6: Stationary monitoring details for Days 3 and 4; Table S7: Apportionment of selected VOCs to the four local factors and the combined background factors for the entire study period (stationary and mobile); Table S8: Apportionment of selected VOCs to the four local factors and the combined background factors for stationary periods only.

Author Contributions: Conceptualization, R.M.H. and U.M.S.; methodology, R.M.H., Q.C., U.M.S. and J.M.W.; software, J.M.W. and U.M.S.; validation, R.M.H., J.M.W. and U.M.S.; formal analysis, R.M.H., U.M.S. and J.M.W.; investigation, R.M.H. and Q.C.; resources, A.T.; data curation, J.M.W.; writing—original draft preparation, R.M.H. and U.M.S.; writing—review and editing, J.M.W., Q.C. and A.T.; visualization, R.M.H. and J.M.W.; supervision, A.T.; project administration, A.T. All authors have read and agreed to the published version of the manuscript.

Funding: This research received no external funding.

Institutional Review Board Statement: Not applicable.

Informed Consent Statement: Not applicable.

Data Availability Statement: Relevant data can be found at the repository for the MOOSE study <https://www-air.larc.nasa.gov/missions/moose/index.html> (accessed on 16 August 2022) or requested from the corresponding author.

Acknowledgments: We would like to acknowledge the technical expertise of George Rioual, who was instrumental in the design and customization of the mobile platform described here. We thank Tony Munoz and Chris Charron for their support with the procurement and development of the mobile platform. We also appreciate the valuable advice and insight on local sources in the study area provided by Sean Morrison, Peder Garber, Peter Rehbein, Jackie Mallott, Greg Heath and Amanda Graham.

Conflicts of Interest: The authors declare no conflict of interest.

References

1. Kansal, A. Sources and Reactivity of NMHCs and VOCs in the Atmosphere: A Review. *J. Hazard. Mater.* **2009**, *166*, 17–26. [CrossRef] [PubMed]
2. McDonald, B.C.; de Gouw, J.A.; Gilman, J.B.; Jathar, S.H.; Akherati, A.; Cappa, C.D.; Jimenez, J.L.; Lee-Taylor, J.; Hayes, P.L.; McKeen, S.A.; et al. Volatile Chemical Products Emerging as Largest Petrochemical Source of Urban Organic Emissions. *Science* **2018**, *359*, 760. [CrossRef]
3. Gkatzelis, G.I.; Coggon, M.M.; McDonald, B.C.; Peischl, J.; Aikin, K.C.; Gilman, J.B.; Trainer, M.; Warneke, C. Identifying Volatile Chemical Product Tracer Compounds in U.S. Cities. *Environ. Sci. Technol.* **2021**, *55*, 188–199. [CrossRef] [PubMed]
4. Seinfeld, J.H.; Pandis, S.N. *Atmospheric Chemistry and Physics: From Air Pollution to Climate Change*; John Wiley & Sons: New York, NY, USA, 1998.
5. Jia, C.; Batterman, S.; Godwin, C. VOCs in Industrial, Urban and Suburban Neighborhoods, Part 1: Indoor and Outdoor Concentrations, Variation, and Risk Drivers. *Atmos. Environ.* **2008**, *42*, 2083–2100. [CrossRef]
6. Hallquist, M.; Wenger, J.C.; Baltensperger, U.; Rudich, Y.; Simpson, D.; Claeys, M.; Dommen, J.; Donahue, N.M.; George, C.; Goldstein, A.H.; et al. The Formation, Properties and Impact of Secondary Organic Aerosol: Current and Emerging Issues. *Atmos. Chem. Phys.* **2009**, *9*, 5155–5235. [CrossRef]
7. Warneke, C.; Geiger, F.; Edwards, P.M.; Dube, W.; Pétron, G.; Kofler, J.; Zahn, A.; Brown, S.S.; Graus, M.; Gilman, J.B.; et al. Volatile Organic Compound Emissions from the Oil and Natural Gas Industry in the Uintah Basin, Utah: Oil and Gas Well Pad Emissions Compared to Ambient Air Composition. *Atmos. Chem. Phys.* **2014**, *14*, 10977–10988. [CrossRef]
8. Liggio, J.; Li, S.-M.; Hayden, K.; Taha, Y.M.; Stroud, C.; Darlington, A.; Drollette, B.D.; Gordon, M.; Lee, P.; Liu, P.; et al. Oil Sands Operations as a Large Source of Secondary Organic Aerosols. *Nature* **2016**, *534*, 91–94. [CrossRef]
9. USEPA Initial List of Hazardous Air Pollutants with Modifications. 2022. Available online: <https://www.epa.gov/haps/initial-list-hazardous-air-pollutants-modifications> (accessed on 19 October 2022).
10. UNECE 1999 Protocol to Abate Acidification, Eutrophication and Ground-Level Ozone to the Convention on Long-Range Transboundary Air Pollution, as Amended on 4 May 2012. 2013. Available online: <https://unece.org/environment-policy/air/protocol-abate-acidification-eutrophication-and-ground-level-ozone> (accessed on 9 April 2021).
11. ECCC Environment and Climate Change Canada 1990–2016 Air Pollutant Emission Inventory Report. 2016. Available online: https://publications.gc.ca/collections/collection_2018/eccc/en81-26-2016-eng.pdf (accessed on 13 April 2021).
12. Miller, L.; Xu, X.; Luginaah, I. Spatial Variability of Volatile Organic Compound Concentrations in Sarnia, Ontario, Canada. *J. Toxicol. Env. Health A* **2009**, *72*, 610–624. [CrossRef]
13. Stroud, C.A.; Zaganescu, C.; Chen, J.; McLinden, C.A.; Zhang, J.; Wang, D. Toxic Volatile Organic Air Pollutants across Canada: Multi-Year Concentration Trends, Regional Air Quality Modelling and Source Apportionment. *J. Atmos. Chem.* **2016**, *73*, 137–164. [CrossRef]
14. Li, S.-M.; Leithead, A.; Moussa, S.G.; Liggio, J.; Moran, M.D.; Wang, D.; Hayden, K.; Darlington, A.; Gordon, M.; Staebler, R.; et al. Differences between Measured and Reported Volatile Organic Compound Emissions from Oil Sands Facilities in Alberta, Canada. *Proc. Natl. Acad. Sci. USA* **2017**, *114*, E3756. [CrossRef]
15. Bari, M.A.; Kindzierski, W.B. Ambient Volatile Organic Compounds (VOCs) in Calgary, Alberta: Sources and Screening Health Risk Assessment. *Sci. Total Environ.* **2018**, *631–632*, 627–640. [CrossRef]
16. Wren, S.N.; Mihele, C.M.; Lu, G.; Jiang, Z.; Wen, D.; Hayden, K.; Mittermeier, R.L.; Staebler, R.M.; Cober, S.G.; Brook, J.R. Improving Insights on Air Pollutant Mixtures and Their Origins by Enhancing Local Monitoring in an Area of Intensive Resource Development. *Environ. Sci. Technol.* **2020**, *54*, 14936–14945. [CrossRef]
17. Xiong, Y.; Du, K. Source-Resolved Attribution of Ground-Level Ozone Formation Potential from VOC Emissions in Metropolitan Vancouver, BC. *Sci. Total Environ.* **2020**, *721*, 137698. [CrossRef]
18. Xiong, Y.; Bari, M.A.; Xing, Z.; Du, K. Ambient Volatile Organic Compounds (VOCs) in Two Coastal Cities in Western Canada: Spatiotemporal Variation, Source Apportionment, and Health Risk Assessment. *Sci. Total Environ.* **2020**, *706*, 135970. [CrossRef]

19. Paatero, P.; Tapper, U. Positive Matrix Factorisation- a Nonnegative Factor Model with Optimal Utilisation of Error-Estimates of Data Values. *Environmetrics* **1994**, *5*, 111–126. [CrossRef]
20. Song, Y.; Shao, M.; Liu, Y.; Lu, S.; Kuster, W.; Goldan, P.; Xie, S. Source Apportionment of Ambient Volatile Organic Compounds in Beijing. *Environ. Sci. Technol.* **2007**, *41*, 4348–4353. [CrossRef]
21. Vlasenko, A.; Slowik, J.G.; Bottenheim, J.W.; Brickell, P.C.; Chang, R.Y.-W.; Macdonald, A.M.; Shantz, N.C.; Sjostedt, S.J.; Wiebe, H.A.; Leaitch, W.R.; et al. Measurements of VOCs by Proton Transfer Reaction Mass Spectrometry at a Rural Ontario Site: Sources and Correlation to Aerosol Composition. *J. Geophys. Res. Atmos.* **2009**, *114*. [CrossRef]
22. Bon, D.M.; Ulbrich, I.M.; de Gouw, J.A.; Warneke, C.; Kuster, W.C.; Alexander, M.L.; Baker, A.; Beyersdorf, A.J.; Blake, D.; Fall, R.; et al. Measurements of Volatile Organic Compounds at a Suburban Ground Site (T1) in Mexico City during the MILAGRO 2006 Campaign: Measurement Comparison, Emission Ratios, and Source Attribution. *Atmos. Chem. Phys.* **2011**, *11*, 2399–2421. [CrossRef]
23. Yuan, B.; Shao, M.; de Gouw, J.; Parrish, D.D.; Lu, S.; Wang, M.; Zeng, L.; Zhang, Q.; Song, Y.; Zhang, J.; et al. Volatile Organic Compounds (VOCs) in Urban Air: How Chemistry Affects the Interpretation of Positive Matrix Factorization (PMF) Analysis. *J. Geophys. Res. Atmos.* **2012**, *117*, D24302. [CrossRef]
24. Crippa, M.; Canonaco, F.; Slowik, J.G.; El Haddad, I.; DeCarlo, P.F.; Mohr, C.; Heringa, M.F.; Chirico, R.; Marchand, N.; Temime-Roussel, B.; et al. Primary and Secondary Organic Aerosol Origin by Combined Gas-Particle Phase Source Apportionment. *Atmos. Chem. Phys.* **2013**, *13*, 8411–8426. [CrossRef]
25. McCarthy, M.C.; Aklilu, Y.-A.; Brown, S.G.; Lyder, D.A. Source Apportionment of Volatile Organic Compounds Measured in Edmonton, Alberta. *Atmos. Environ.* **2013**, *81*, 504–516. [CrossRef]
26. Dumanoglu, Y.; Kara, M.; Altioik, H.; Odabasi, M.; Elbir, T.; Bayram, A. Spatial and Seasonal Variation and Source Apportionment of Volatile Organic Compounds (VOCs) in a Heavily Industrialized Region. *Atmos. Environ.* **2014**, *98*, 168–178. [CrossRef]
27. Rocco, M.; Colomb, A.; Baray, J.-L.; Amelynck, C.; Verreyken, B.; Borbon, A.; Pichon, J.-M.; Bouvier, L.; Schoon, N.; Gros, V.; et al. Analysis of Volatile Organic Compounds during the OCTAVE Campaign: Sources and Distributions of Formaldehyde on Reunion Island. *Atmosphere* **2020**, *11*, 140. [CrossRef]
28. Gkatzelis, G.I.; Coggon, M.M.; McDonald, B.C.; Peischl, J.; Gilman, J.B.; Aikin, K.C.; Robinson, M.A.; Canonaco, F.; Prevot, A.S.H.; Trainer, M.; et al. Observations Confirm That Volatile Chemical Products Are a Major Source of Petrochemical Emissions in U.S. Cities. *Environ. Sci. Technol.* **2021**, *55*, 4332–4343. [CrossRef] [PubMed]
29. ECCC Environment and Climate Change Canada National Pollutant Release Inventory. 2019. Available online: <https://www.canada.ca/en/environment-climate-change/services/national-pollutant-release-inventory/tools-resources-data/access.html> (accessed on 13 April 2021).
30. Oiamo, T.H.; Luginaah, I.N.; Atari, D.O.; Gorey, K.M. Air Pollution and General Practitioner Access and Utilization: A Population Based Study in Sarnia, “Chemical Valley,” Ontario. *Environ. Health* **2011**, *10*, 71. [CrossRef]
31. Jordan, A.; Haidacher, S.; Hanel, G.; Hartungen, E.; Märk, L.; Seehauser, H.; Schottkowsky, R.; Sulzer, P.; Märk, T.D. A High Resolution and High Sensitivity Proton-Transfer-Reaction Time-of-Flight Mass Spectrometer (PTR-TOF-MS). *Int. J. Mass Spectrom.* **2009**, *286*, 122–128. [CrossRef]
32. Baudic, A.; Gros, V.; Sauvage, S.; Locoge, N.; Sanchez, O.; Sarda-Estève, R.; Kalogridis, C.; Petit, J.-E.; Bonnaire, N.; Baisnée, D.; et al. Seasonal Variability and Source Apportionment of Volatile Organic Compounds (VOCs) in the Paris Megacity (France). *Atmos. Chem. Phys.* **2016**, *16*, 11961–11989. [CrossRef]
33. Wang, L.; Slowik, J.G.; Tripathi, N.; Bhattu, D.; Rai, P.; Kumar, V.; Vats, P.; Satish, R.; Baltensperger, U.; Ganguly, D.; et al. Source Characterization of Volatile Organic Compounds Measured by Proton-Transfer-Reaction Time-of-Flight Mass Spectrometers in Delhi, India. *Atmos. Chem. Phys.* **2020**, *20*, 9753–9770. [CrossRef]
34. Li, H.; Canagaratna, M.R.; Riva, M.; Rantala, P.; Zhang, Y.; Thomas, S.; Heikkinen, L.; Flaud, P.-M.; Villenave, E.; Perraudin, E.; et al. Atmospheric Organic Vapors in Two European Pine Forests Measured by a Vocus PTR-TOF: Insights into Monoterpene and Sesquiterpene Oxidation Processes. *Atmos. Chem. Phys.* **2021**, *21*, 4123–4147. [CrossRef]
35. Tan, Y.; Han, S.; Chen, Y.; Zhang, Z.; Li, H.; Li, W.; Yuan, Q.; Li, X.; Wang, T.; Lee, S. Characteristics and Source Apportionment of Volatile Organic Compounds (VOCs) at a Coastal Site in Hong Kong. *Sci. Total Environ.* **2021**, *777*, 146241. [CrossRef]
36. Yang, Y.; Liu, B.; Hua, J.; Yang, T.; Dai, Q.; Wu, J.; Feng, Y.; Hopke, P.K. Global Review of Source Apportionment of Volatile Organic Compounds Based on Highly Time-Resolved Data from 2015 to 2021. *Environ. Int.* **2022**, *165*, 107330. [CrossRef]
37. Majluf, F.Y.; Krechmer, J.E.; Daube, C.; Knighton, W.B.; Dyroff, C.; Lambe, A.T.; Fortner, E.C.; Yacovitch, T.I.; Roscioli, J.R.; Herndon, S.C.; et al. Mobile Near-Field Measurements of Biomass Burning Volatile Organic Compounds: Emission Ratios and Factor Analysis. *Environ. Sci. Technol. Lett.* **2022**, *9*, 383–390. [CrossRef]
38. Norris, G.; Duvall, R.; Brown, S.; Bai, S. EPA Positive Matrix Factorization (PMF) 5.0 Fundamentals and User Guide. 2014. Available online: https://www.epa.gov/sites/default/files/2015-02/documents/pmf_5.0_user_guide.pdf (accessed on 15 July 2022).
39. Paatero, P. The Multilinear Engine—a Table-Driven, Least Squares Program for Solving Multilinear Problems, Including the n-Way Parallel Factor Analysis Model. *J. Comput. Graph. Stat.* **1999**, *8*, 854–888.
40. Slowik, J.G.; Vlasenko, A.; McGuire, M.; Evans, G.J.; Abbatt, J.P.D. Simultaneous Factor Analysis of Organic Particle and Gas Mass Spectra: AMS and PTR-MS Measurements at an Urban Site. *Atmos. Chem. Phys.* **2010**, *10*, 1969–1988. [CrossRef]

41. Sofowote, U.M.; Su, Y.; Dabek-Zlotorzynska, E.; Rastogi, A.K.; Brook, J.; Hopke, P.K. Constraining the Factor Analytical Solutions Obtained from Multiple-Year Receptor Modeling of Ambient PM_{2.5} Data from Five Speciation Sites in Ontario, Canada. *Atmos. Environ.* **2015**, *108*, 151–157. [[CrossRef](#)]
42. Gueneron, M.; Erickson, M.H.; VanderSchelden, G.S.; Jobson, B.T. PTR-MS Fragmentation Patterns of Gasoline Hydrocarbons. *Int. J. Mass Spectrom.* **2015**, *379*, 97–109. [[CrossRef](#)]
43. Erickson, M.H.; Gueneron, M.; Jobson, B.T. Measuring Long Chain Alkanes in Diesel Engine Exhaust by Thermal Desorption PTR-MS. *Atmos. Meas. Tech.* **2014**, *7*, 225–239. [[CrossRef](#)]
44. Healy, R.M.; Chen, Q.; Bennett, J.; Karellas, N.S. A Multi-Year Study of VOC Emissions at a Chemical Waste Disposal Facility Using Mobile APCI-MS and LPCI-MS Instruments. *Environ. Pollut.* **2017**, *232*, 220–228. [[CrossRef](#)]
45. ECCC Environment and Climate Change Canada National Air Pollution Surveillance Program. 2022. Available online: <https://www.canada.ca/en/environment-climate-change/services/air-pollution/monitoring-networks-data/national-air-pollution-program.html> (accessed on 6 July 2022).
46. Ashbaugh, L.L.; Malm, W.C.; Sadeh, W.Z. A Residence Time Probability Analysis of Sulfur Concentrations at Grand Canyon National Park. *Atmos. Environ.* (1967) **1985**, *19*, 1263–1270. [[CrossRef](#)]
47. Verreyken, B.; Amelynck, C.; Schoon, N.; Müller, J.-F.; Brioude, J.; Kumps, N.; Hermans, C.; Metzger, J.-M.; Colomb, A.; Stavrakou, T. Measurement Report: Source Apportionment of Volatile Organic Compounds at the Remote High-Altitude Maïdo Observatory. *Atmos. Chem. Phys.* **2021**, *21*, 12965–12988. [[CrossRef](#)]
48. Read, K.A.; Carpenter, L.J.; Arnold, S.R.; Beale, R.; Nightingale, P.D.; Hopkins, J.R.; Lewis, A.C.; Lee, J.D.; Mendes, L.; Pickering, S.J. Multiannual Observations of Acetone, Methanol, and Acetaldehyde in Remote Tropical Atlantic Air: Implications for Atmospheric OVOC Budgets and Oxidative Capacity. *Environ. Sci. Technol.* **2012**, *46*, 11028–11039. [[CrossRef](#)] [[PubMed](#)]
49. Loomis, D.; Guyton, K.Z.; Grosse, Y.; El Ghissassi, F.; Bouvard, V.; Benbrahim-Tallaa, L.; Guha, N.; Vilahur, N.; Mattock, H.; Straif, K. Carcinogenicity of Benzene. *Lancet Oncol.* **2017**, *18*, 1574–1575. [[CrossRef](#)]